Coalescence in Surfactant-Stabilized Double Emulsions

ARTICLE *in* LANGMUIR · NOVEMBER 2001

Impact Factor: 4.46 · DOI: 10.1021/la010735x

5 AUTHORS, INCLUDING:

Joanna Giermanska
French National Centre for Scientific Research
35 PUBLICATIONS **743** CITATIONS
SEE PROFILE

Bernard Pouligny
Centre de Recherche Paul Pascal
87 PUBLICATIONS **1,562** CITATIONS
SEE PROFILE

Coalescence in Surfactant-Stabilized Double Emulsions

K. Pays, J. Giermanska-Kahn, B. Pouligny, J. Bibette,† and F. Leal-Calderon*

Centre de Recherche Paul Pascal, CNRS, Avenue Schweitzer, 33600 Pessac, France, and ESPCI, Laboratoire "Colloïdes et Nanostructures", UMR 7612, 10 Rue Vauquelin, 75005 Paris, France

Received May 17, 2001. In Final Form: August 3, 2001

In this paper, we investigate the two mechanisms that are responsible for the release of a chemical substance from water-in-oil-in-water double emulsions. (i) One is due to the coalescence of the thin liquid film separating the internal droplets and the oil globule surface. (ii) The other mechanism occurs without film rupturing, that is, by diffusion and/or permeation of the chemical substance across the oil phase. The thin liquid film that forms between the internal droplets and the globule surface is composed of two mixed monolayers covered by hydrophilic and hydrophobic surfactant molecules. Following the well-known Bancroft rule, such inverted films possess a long-range stability with respect to coalescence when essentially covered by hydrophobic surfactant. In that limit, the release is governed by diffusion and/or permeation. However, the film becomes very unstable when a strong proportion of hydrophilic surfactant is adsorbed and the release is then controlled by coalescence. We show that the transition from one regime (diffusion) to the other (coalescence) may be achieved by varying the concentration of the hydrophilic surfactant in the external water phase. We study the kinetics of release in the regime dominated by coalescence, and we propose an unambiguous method for the measurement of the microscopic parameters implied in liquid film rupturing. Our method exploits the fact that the total number of internal droplets adsorbed on the globule surface governs the rate of release. At low internal droplet volume fraction, measuring the rate of release allows a direct determination of the average lifetime of the thin film that forms between the small internal droplet and the globule surface. We deduce the activation energy and the natural frequency of the coalescence process by exploring the temperature dependence of the rate of release.

I. Introduction

Water-in-oil-in-water double emulsions (W/O/W) consist of dispersed oily globules containing smaller aqueous droplets. Taking advantage of their double (or multiple) compartment structure, an increasing interest has been devoted to double emulsions, since their first description in 1925,[1] as they can be considered as reservoirs of encapsulated substances to be released under variable conditions. The industrial domains showing interest toward the technological development of such complex systems are various. One can list the food industry, with its research in new "light" products, that is, with reduced amounts of fat substances or in taste-masking, and the cosmetic industry, with prolonged efficiency products which would ideally contain water-soluble active ingredients. Products formulated as multiple emulsions may also be very appreciated in other domains such as agriculture and housekeeping. Probably the major part of applications concerns the human pharmaceutical field: W/O/W emulsions have mostly been investigated as potential vehicles for various hydrophilic drugs (vaccines, vitamins, enzymes, and hormones) which would be then progressively released. Active substances may also migrate from the outer to the inner phase of a multiple emulsion, providing in that case a kind of reservoir particularly suitable for detoxification (overdose treatment) or, in an again different domain, in the removal of toxic materials from wastewater. Anyway, the impact of double emulsions designed as drug delivery systems would be then of significant importance in the controlled release field, for oral, topical, or parenteral administrations, provided that the stability and release mechanisms may be more clearly understood and monitored.

Double emulsions are generally prepared with two surfactants of opposite solubility. To produce a W/O/W emulsion, a low hydrophilic−lipophilic balance (HLB) (<10) surfactant is first dissolved in oil. Then, water is added and a W/O emulsion is formed. The system is then emulsified again in an aqueous solution of surfactant with a high HLB number (>10) to produce a W/O/W double emulsion. Both surfactants mix at the water/oil interfaces, and the lifetime of the films is governed by the composition of the binary surfactant mixture. Different authors have already explored the role of the hydrophobic and hydrophilic emulsifiers on the release properties and proposed some mechanistic interpretations.[2−4] However, double emulsions still raise many questions concerning the microscopic phenomena involved in the release process.

In this paper, we investigate the two mechanisms that are responsible for the release of a chemical substance. (i) One is due to the coalescence of the thin liquid film separating the internal droplets and the globule surfaces. (ii) The other mechanism termed as "compositional ripening" occurs without film rupturing; instead, it occurs by diffusion and/or permeation of the chemical substance across the oil phase. By associating water- and oil-soluble surfactants in appropriate proportions, we found experimental conditions where the release is only due to coalescence. This mechanism was experimentally studied allowing a measurement of the microscopic parameters implied in liquid film rupturing (activation energy and natural hole nucleation frequency). We finally conclude

* Corresponding author. Tel: (33) 5 56 84 56 33. Fax: (33) 5 56 84 56 00. E-mail: leal@crpp.u-bordeaux.fr.

† ESPCI, Laboratoire "Colloïdes et Nanostructures".

(1) Seifriz, W. *J. Phys. Chem.* **1925**, *29*, 738.

(2) Matsumoto, S.; Kang, W. W. *J. Dispersion Sci. Technol.* **1989**, *10*, 455.

(3) Magdassi, S.; Garti, N. *J. Controlled Release* **1986**, *3*, 273.

(4) Garti, N. *Colloids Surf.* **1997**, *123*, 233.

10.1021/la010735x CCC: $20.00
Published on Web 11/08/2001

about the ability of short surfactants to ensure long-term encapsulation.

II. Experimental Section

1. Emulsion Preparation. For the oil phase, we used alkane oils such as octane, dodecane, and hexadecane (from Aldrich). To stabilize inverted W/O emulsions, an oil-soluble surfactant was employed: Span 80 (sorbitan monooleate) from Aldrich with HLB = 4. To stabilize direct O/W emulsions, we choose different hydrophilic surfactants such as sodium dodecyl sulfate (or SDS, HLB = 40), all of them purchased from Aldrich.

W/O/W monodisperse emulsions are fabricated following a two-step procedure.

a. Preparation of the Primary W/O Emulsion. We first prepare a monodisperse water-in-oil inverted emulsion, stabilized by an oil-soluble surfactant. The initial step consists of preparing a crude polydisperse emulsion, the so-called premixed emulsion. It is obtained by incorporating the dispersed phase under very gentle stirring in order to avoid the formation of small droplets. Salt is added to the dispersed phase as a tracer to probe the release mechanisms but also to avoid the coarsening phenomena.[5] A Couette-type mixer consisting of two concentric cylinders was used for emulsion fabrication. A scheme of the setup is available in ref 6. The inner cylinder of radius $r \approx 20$ mm is moved by a motor that rotates at a selected angular velocity ω which can reach up to 70 rad s^{-1}. The outer cylinder is immobile. The gap between the stator and the rotor is fixed to $e = 100\ \mu$m. For the maximum angular velocity, we are able to reach very high shear rates $\dot{\gamma} \approx r\omega/e = 14\ 200\ s^{-1}$ in simple shear flow conditions. The premixed crude emulsion is pushed into the gap between the rotor and the stator by means of a piston, and the residence time of the emulsion inside the mixer gap is of the order of 10 s. With this Couette mixer, it is possible to produce significant quantities of emulsions with very narrow size distribution (up to 1 L/h, depending on the system, at volume fractions ranging from 70 to 90%). After emulsification, the lipophilic surfactant concentration with respect to the continuous phase is always fixed at a given value C_l and the water droplet volume fraction is set to a given value ϕ_i^0. This is obtained by centrifugating the inverted emulsion, removing the continuous phase, and replacing it by a surfactant solution at concentration C_l. This washing procedure is repeated at least three times in order to set precisely the composition at the desired value.

b. Preparation of the Double W/O/W Emulsion. The double emulsion is fabricated by dispersing the inverted one within an aqueous continuous phase containing a very low concentration of hydrophilic surfactant[7] (typically cmc/100, where cmc is the critical micellar concentration; in the following and in the absence of any other indication, cmc will always refer to the value measured in pure water). Also, glucose is added in order to avoid any osmotic pressure mismatch between the internal and the external water compartments. In this second step, we use the high-pressure jet homogenizer JH-1 (LabPlant Ltd, U.K.). We obtain double globules (volume fraction ϕ_g) with a very narrow size distribution. Right after preparation, some hydrophilic surfactant is added to the external water continuous phase up to a given value C_h. Figure 1 shows a microscopic picture of a double emulsion stabilized with SDS at concentration C_h = cmc/10 (cmc = 8×10^{-3} mol/L), right after fabrication at room temperature (glucose concentration = 11.5% (w/w) which matches the osmotic pressure of the internal droplets containing 0.4 M NaCl [from *Handbook of Chemistry*]). Large oil globules (around 10 μm) are visible, each one containing smaller inverted water droplets.

2. Emulsion Characterization. The emulsions are observed with a phase contrast optic microscope (Zeiss, Axiovert X100). Since the double emulsions possess a very narrow size distribution, it is easy to determine the average globule diameter from microscopic images. We also used a Malvern Mastersizer granulometer to measure the size distribution of the emulsions. The collected scattered intensity as a function of the angle is transformed into the size distribution using the Mie theory. The mean droplet size in volume $D(4,3)$ is defined as

$$D(4,3) = \frac{\sum_i N_i D_i^4}{\sum_i N_i D_i^3}$$

where N_i is the total number of droplets with diameter D_i. The polydispersity of the emulsion is characterized by a parameter termed as "uniformity" and defined as

$$U = \frac{1}{\overline{D}} \frac{\sum_i N_i D_i^3 |\overline{D} - D_i|}{\sum_i N_i D_i^3}$$

where $\overline{D}$ is the median diameter, that is, the diameter for which the cumulative undersized volume fraction is equal to 50%. In the following, we shall characterize the obtained emulsions through $D(4,3)$ and U. Here, it is important to stress that in the special case of double emulsions, the scattering objects are optically nonuniform. Indeed, the double globules contain small water droplets with a characteristic size close to the wavelength of the laser beam. The scattering properties of such complex objects are not considered in the software of our commercial granulometer. We therefore decided to use Mie theory assuming that the double globules optically behave like simple droplets, with the same refractive index as the oil phase. This approximation, although questionable, was revealed to be quite satisfactory. Indeed, for each sample we checked that the average diameter $D(4,3)$ was very close to the one directly obtained from direct microscopic observations. In Figure 2, we plot two characteristic size distributions, one corresponding to a primary W/O emulsion and the other one corresponding to a double W/O/W emulsion. In both cases, the uniformity U is lower than 30%. In comparison with previous studies,[2−4] our systems possess the advantage of being well calibrated and reproducible. This is an important property since, as will be demonstrated in this paper, the rate of release of double emulsions is strongly dependent upon the colloidal size of the dispersed objects.

In the following, we shall systematically use the following notations to characterize the double emulsion composition and properties: C_l = concentration of the lipophilic surfactant in the oil globules; C_h = initial concentration of the hydrophilic

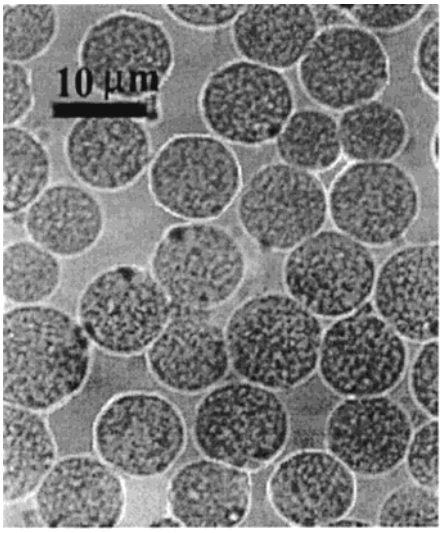

Figure 1. Microscopic image obtained following the two-step procedure described in the text. $d_g = 9\ \mu$m, $d_i = 0.36\ \mu$m, $\phi_i = 20\%$, $\phi_g = 10\%$, $C_h = 0.1$ cmc.

(5) Aronson, M. P.; Petko, M. F. *J. Colloid Interface Sci.* **1993**, *159*, 134.

(6) Mabille, C.; Schmitt, V.; Gorria, P.; Leal-Calderon, F.; Faye, V.; Deminière, B.; Bibette, J. *Langmuir* **2000**, *16*, 422.

(7) Pays, K.; Leal-Calderon, F.; Bibette, J. French Patent, CNRS, No. 00 05880.

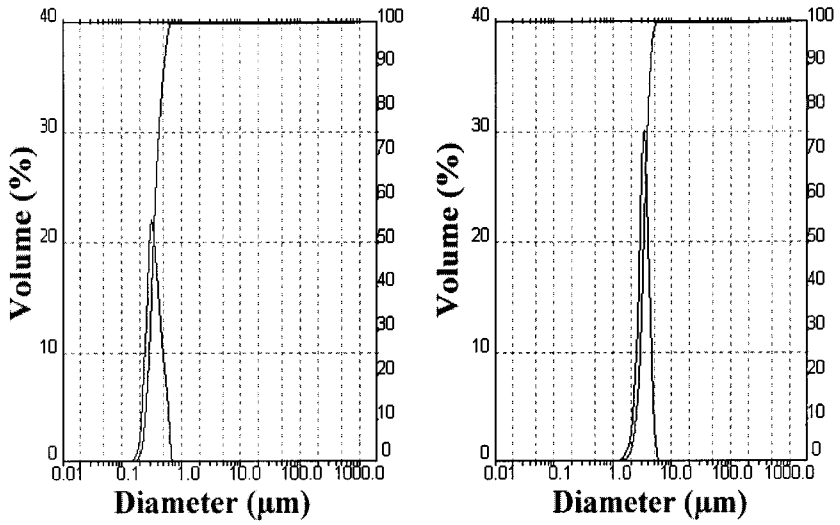

Figure 2. (a) Size distribution of an inverted W/O emulsion; $D(4,3) = 0.36\ \mu$m, $U = 0.23$. (b) Size distribution of a double emulsion; $D(4,3) = 3.35\ \mu$m, $U = 0.16$.

surfactant in the external water phase; ϕ_i = volume fraction of water droplets in the oil globules; ϕ_g = volume fraction of oil globules in the external water phase; d_i = diameter of the water droplets; d_g = diameter of the oil globules.

3. Techniques to Follow the Kinetics of Release. We used different techniques to study the kinetic evolution of the double emulsions. The concentration of salt (NaCl) present in the aqueous external phase is measured by means of an Ag/AgCl specific electrode (from Radiometer, France) which is sensitive to the chemical activity of chloride ions. The measured potential is transformed into the salt concentration using a calibration curve. The emulsion is very gently stirred (maximum 60 rpm) in order to avoid the creaming of the oil globules and any nonhomogeneous distribution of the salt concentration. We verified that this slow rate of stirring does not perturb the rate of release. We combined this technique with direct observations under microscope (Axiovert X100) as well as repeated single globule creaming experiments using optical manipulation. In our setup, a unique non-Brownian globule (more than 10 μm in diameter) is illuminated by one or two moderately focused laser beams.[8] The radiation pressure exerted by the lasers allows capture and displacement of a globule at any position in a transparent cell. When the lasers are switched off, the globule moves up because of buoyancy. We then measure under the microscope the globule radius R as well as its creaming velocity $V_{creaming}$ in the stationary regime. From the Stokes equation, we deduce the average density of the globule ρ_g:

$$V_{creaming} = \frac{2}{9}\frac{(\rho_w - \rho_g)gR^2}{\eta_c} \quad (1)$$

In eq 1, ρ_w is the density of the water phase, g is the acceleration of gravity (9.8 m s^{-2}), and η_c is the continuous phase viscosity. It then becomes possible to determine the internal droplet volume fraction ϕ_i inside the globules according to the relation

$$\rho_g = \phi_i\rho_{wi} + (1 - \phi_i)\rho_o \quad (2)$$

where ρ_o is the oil density and ρ_{wi} is the density of the internal water phase.

III. Results

1. General Phenomenology. A diagram representing the behavior of calibrated double emulsions is drawn in Figure 3. In (C_h, ϕ_i^0) coordinates, we can define three

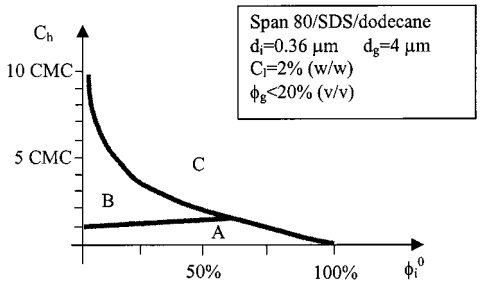

Figure 3. Behavior of a quasi-monodisperse double emulsion as a function of two initial composition parameters C_h and ϕ_i^0. Observations are performed under the microscope during 24 h after preparation: A, no coalescence at all; B, droplet−globule coalescence; C, droplet−droplet and droplet−globule coalescence.

different compositions zones A, B, and C where the qualitative behavior observed under the microscope is different. Span 80 is used for the stabilization of the primary W/O emulsion at concentration C_l = 2% (w/w) with respect to the continuous phase. The internal droplets have a diameter $d_i = 0.36\ \mu$m with a uniformity of 30%. We first consider a quasi-monodisperse double emulsion with moderate internal droplet and globule volume fractions ($\phi_i^0 < 20\%$, $\phi_g < 20\%$). If the double globules are stabilized in water by SDS at cmc/10, the system does not exhibit any structural evolution after a few days of storage (zone A). However, if the SDS concentration is equal to or larger than approximately 1 cmc, the double W/O/W emulsion rapidly transforms into a simple O/W emulsion (see Figure 4). The characteristic time scale for the transformation becomes shorter when the SDS concentration increases, in perfect agreement with the pioneering experiments of Ficheux et al.[9] For globules with diameter $d_g = 4\ \mu$m, $\phi_i^0 = 5\%$, and $C_h = 10$ cmc, it takes around 300 min for the transformation to occur. Repeated observations under the microscope reveal that the globules become progressively empty and that there is apparently no coarsening of the internal droplets (zone B). To elucidate the origin of this evolution, we produce polydisperse double

(8) Ashkin, A. *Phys. Rev. Lett.* **1970**, *24*, 156. Angelova, M. I.; Pouligny, B. *Pure Appl. Opt.* **1993**, *2*, 261.

(9) Ficheux, M. F.; Bonakdar, L.; Leal-Calderon, F.; Bibette, J. *Langmuir* **1998**, *14*, 2702.

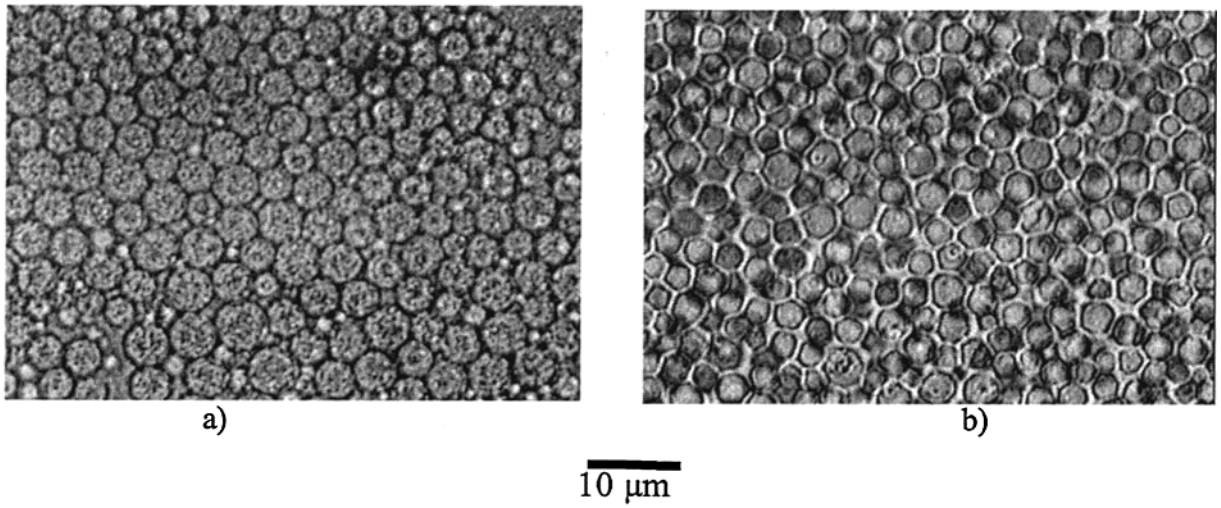

Figure 4. Transformation of an emulsion from double to simple. $C_h = 10$ cmc.

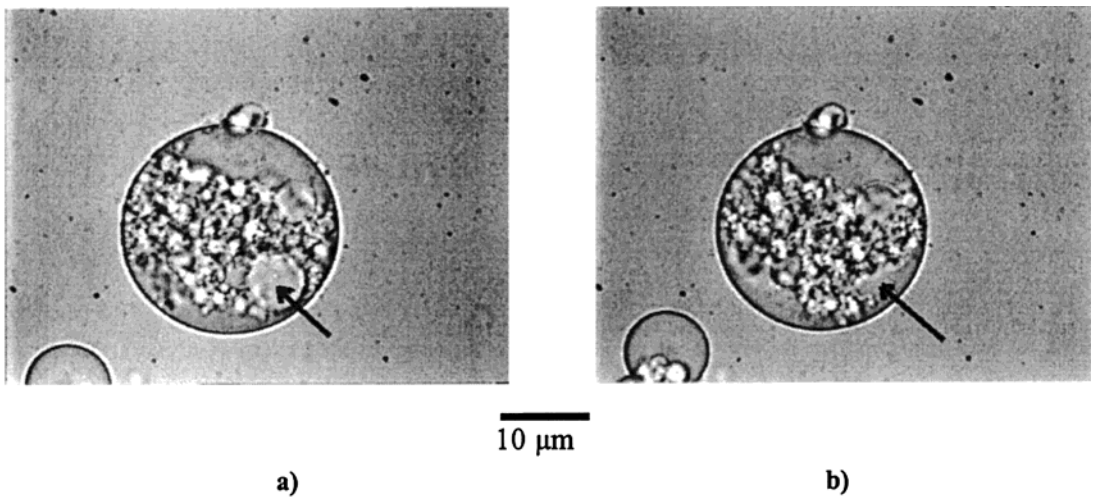

Figure 5. The internal droplet indicated by the arrow coalesces on the globule surface. The two images are taken at a 1 s interval.

emulsions with large internal droplets that can be perfectly distinguished under the microscope. Within the same conditions, we observe that the internal droplets may spend some time in contact with the globule surface without exhibiting any structural change and then suddenly disappear as shown in Figure 5. From all the previous observations, it can be concluded that the mechanism responsible for the transformation from double to simple emulsion is the coalescence of the internal droplets on the globule surface.

A slightly distinct scenario of destruction occurs when the initial droplet volume fraction ϕ_i^0 exceeds some critical value that depends on C_h. The transition from double to simple emulsion is still observed, but in this case there is some coarsening of the internal droplets during the process of destruction (zone C in Figure 3). This is visible in the images of Figure 6, taken at regular time intervals. Some large nuclei resulting from droplet−droplet coalescence are clearly distinguished under the microscope. Once they reach the surface, they coalesce rapidly and disappear. In the last stages of the transformation, when the droplet concentration becomes small enough, we no longer observe the coarsening and the scenario becomes identical to the one observed for the systems with low initial droplet concentration (Figure 6c).

In the case of extremely concentrated droplets ($\phi_i^0 > 90$), the destruction permanently involves droplet−droplet and droplet−globule coalescence. Figure 7 is a sequence showing the destruction of a single globule as a function of time. To facilitate the observation, we consider here a very large globule with initial diameter around 30 μm. The optical contrast between the globule initially containing 95% (v/v) water and the aqueous external phase is quite low, which explains the difficulty in discerning the globule. The globule diameter rapidly decreases as a consequence of the droplet−globule coalescence. On the other hand, the large nuclei observed inside the globules result from droplet−droplet coalescence. The total destruction of the globule at a SDS concentration of 3 cmc occurs over a time scale of the order of 10 min, a much shorter lifetime than for an initially diluted globule.

2. Role of the Hydrophilic Surfactant. The phenomenology described above is general since it was reproduced using different ionic surfactants with high HLB values (>30), like alkyl sulfonates or alkyl quaternary ammonia. It is known that the micellar phase always tends to be the continuous phase of an emulsion. Recently, a mechanistic interpretation for this correlation was proposed, according to which the surfactant packing type (spontaneous curvature) affects both the phase behavior of microemulsions and the coalescence energy barrier of emulsions. Kabalnov and Wennerström[10] argue that the effect of the spontaneous curvature on emulsion stability comes from the kinetics of the hole nucleation in emulsion

(10) Kabalnov, A.; Wennerström, H. *Langmuir* **1996**, *12*, 276.

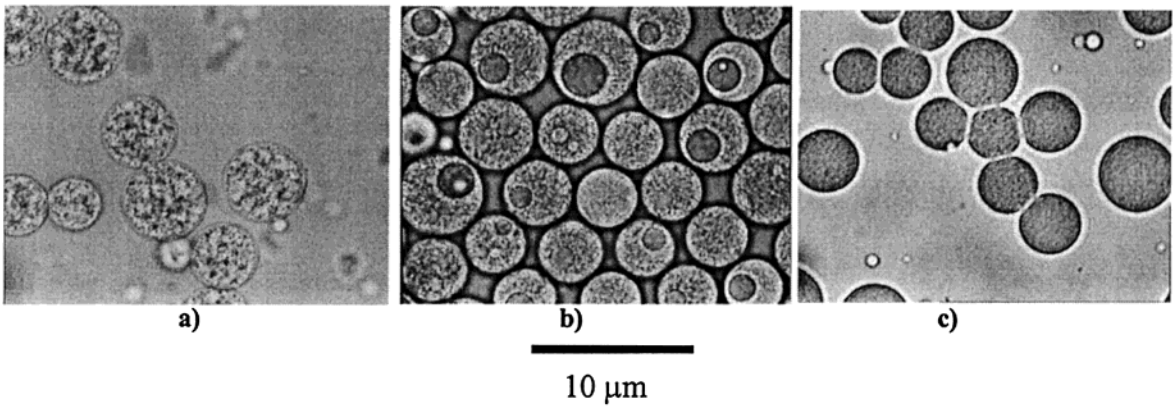

Figure 6. Destruction of a double emulsion with high initial droplet volume fraction. $\phi_i^0 = 50\%$; $C_h = 3$ cmc. (a) $t = 60$ min; (b) $t = 250$ min; (c) $t = 850$ min.

films. Consider an oil film separating an internal water droplet from the external water phase (Figure 8). If the hydrophilic surfactant concentration is low, the monolayer covering the droplet and globule surfaces is essentially composed of Span 80 molecules. The spontaneous curvature of this low HLB surfactant is negative (W/O shape). The propagation of a hole is damped, because the monolayer at the edge of the nucleation hole is frustrated since it is curved against the direction favored by the spontaneous curvature. Because of this, for the film rupture to occur, the system must pass through an energy barrier, after which the growth becomes spontaneous. This state can be reached only by a thermal fluctuation and has a low probability because of the unfavorable spontaneous curvature. However, adding SDS in the external water phase has the effect of concentrating this molecule at the interfaces thus rendering the average spontaneous curvature less negative or even positive. The hole propagation for the W/O/W film occurs with a very moderate energy barrier because the curvature of the edge fits the spontaneous curvature. This could explain why the coalescence of the internal droplets on the globule surface occurs above a critical SDS concentration in the external water phase (around 1 cmc). Since coalescence also occurs between the internal droplets when they are sufficiently concentrated, we deduce that the hydrophilic surfactant initially introduced in the external water phase is being transferred toward the internal droplets as a result of the entropy of mixing.

3. Partitioning of the Hydrophilic Surfactant and Kinetics. We thus designed an experiment devoted to measuring the kinetics of the surfactant transfer. Since SDS is an ionic molecule, its concentration in the external continuous phase can be easily determined from conductometric measurements. The measured conductivity is transformed into concentration via a calibration curve which is established in the presence of the same globules and at the same volume fraction as in double emulsions. We prepare W/O monodisperse emulsion droplets containing 11.5% (w/w) glucose (instead of NaCl to avoid any perturbation of the conductivity measurement). The primary emulsion is dispersed in a SDS (cmc/200) + glucose (11.5% (w/w)) water solution leading to quasi-monodisperse double globules. The exact composition and the structural parameters are given in the caption of Figure 9. Right after preparation, we add SDS in the external phase up to exactly 1 cmc and we immediately measure the conductivity in the external phase. The global composition was chosen so that the internal droplets incorporate approximately half of the total amount of SDS molecules. In such experimental conditions, the SDS concentration is high enough for the conductometric detection to be performed accurately but insufficient to induce the destruction of the double emulsion at the time scale of our experiment (less than 15 min). The conductivity rapidly decreases, and Figure 9 shows the evolution of the equivalent SDS concentration as a function of time. After less than 10 min, the concentration decreases and reaches a plateau value around 0.5 cmc. At the same time, we do not observe under the microscope any coarsening of the emulsion: the internal droplets and globules maintain their initial diameter, and the droplet concentration inside the globules does not seem to vary. The conductivity evolution confirms the fact that the hydrophilic surfactant is transferred from the outer to the inner water phase, and we learn that the rate of the transfer is rapid. From very simple geometrical considerations, we can deduce the total concentration of SDS in the water droplets C_{hi} after equilibration:

$$C_{hi} = \frac{(C_{he}^{\,0} - C_{he})(1 - \phi_g)}{\phi_g \phi_i^{\,0}} \approx 4 \text{ cmc}$$

where $C_{he}^{\,0}$ is the initial concentration in the external phase (1 cmc), and C_{he} is the concentration at equilibrium (≈0.5 cmc). In the above calculation, C_{hi} represents the total concentration of SDS molecules with respect to the droplet volume. However, the concentration may be decomposed in two contributions since a fraction of the SDS is adsorbed on the droplet surface ($C_{hi}^{\,s}$), while the other one is dissolved in the volume of the droplets ($C_{hi}^{\,v}$):

$$C_{hi} = C_{hi}^{\,s} + C_{hi}^{\,v}$$

Assuming that the volume concentration ($C_{hi}^{\,v}$) in the droplets is the same as in the external water phase (≈0.5 cmc), we deduce the SDS surface concentration Γ at the oil−water interface:

$$\Gamma = \frac{d_i}{6} C_{hi}^{\,s}$$

From the numerical data, we obtain a value of 1.3 molecules/nm^2. This is a quite reasonable value assuming that the maximum packing of SDS at the oil−water interface is of the order of 2.5 molecules/nm^2 and considering that Span 80 is also present at the interface.

4. Stability of Simple W/O Inverted Emulsions Containing Hydrophilic Surfactant. We now examine the influence of SDS molecules on the stability of the W/O/W films. For that purpose, we fabricate simple water-

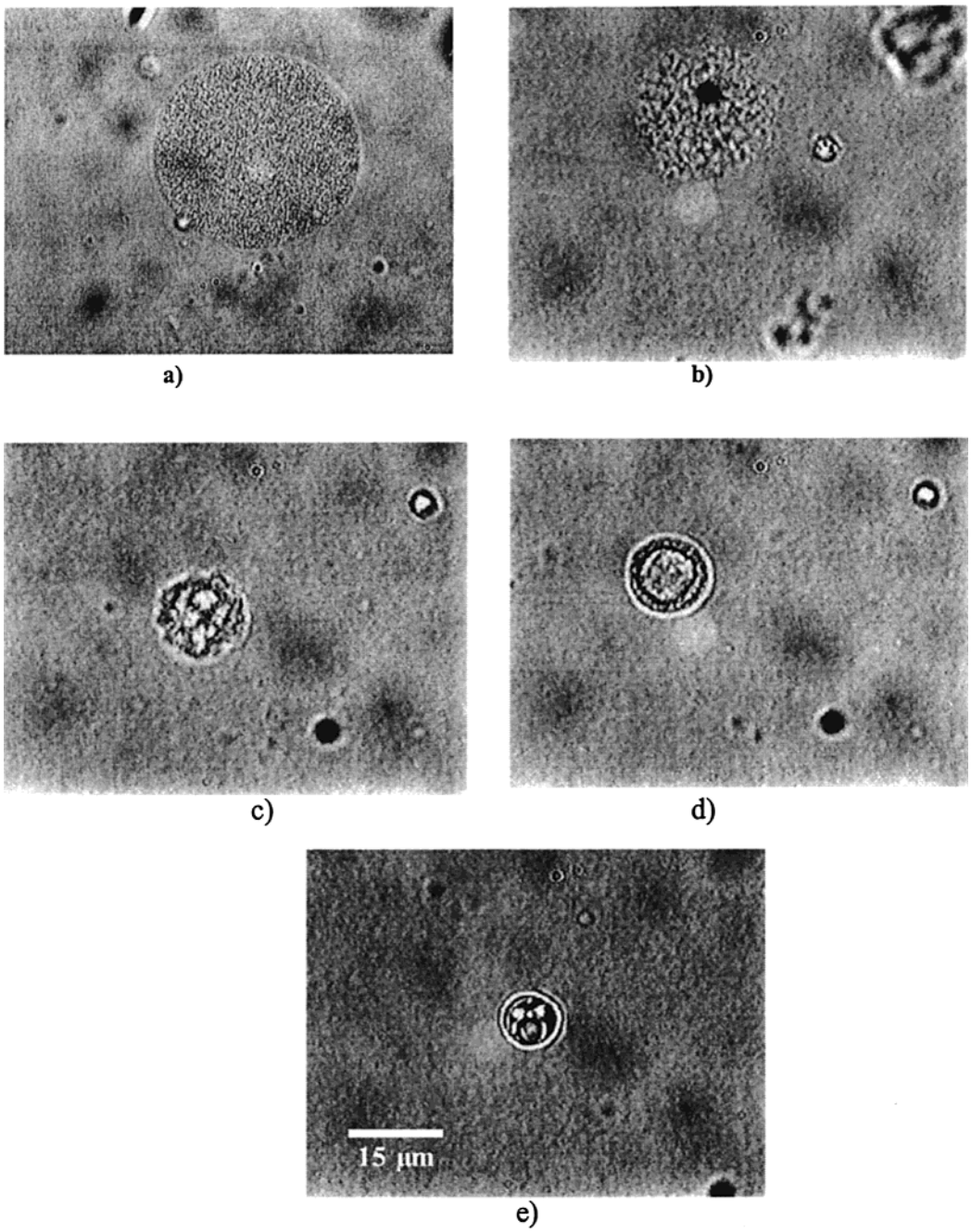

Figure 7. Destruction of a double emulsion with very high initial droplet volume fraction. $\phi_i^0 = 95\%$; $C_h = 3$ cmc. (a) $t = 0$; (b) $t = 26$ s; (c) $t = 2$ min; (d) $t = 7$ min; (e) $t = 10$ min.

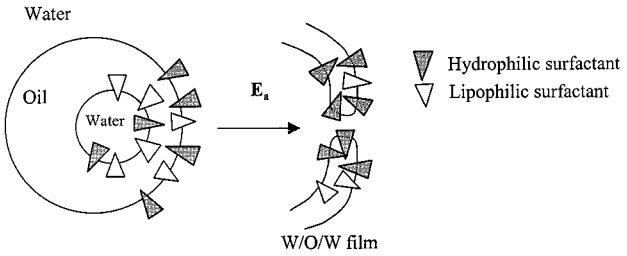

Figure 8. Scheme of the hole nucleation process in a W/O/W film.

in-dodecane inverted emulsions stabilized by Span 80 (2% (w/w)) and we introduce variable amounts of SDS in the water phase prior to the emulsification. The fabrication is performed using the high-pressure jet homogenizer (LabPlant Ltd.) instead of the Couette-type cell in order to avoid phase inversion due to the presence of SDS. All the W/O emulsions are prepared at the same initial water volume fraction (30%) and have the same droplet diameter $d_i = 0.36\ \mu$m with uniformity around 30%. Salt (NaCl 0.4 M) is dissolved in the droplets in order to stabilize them against Oswald ripening. To compare their relative stability, the emulsions are centrifuged at 140 000*g* and we measure the height of the clear water layer coalesced at the bottom of the centrifugation tubes. In Figure 10, we plot the relative height of the coalesced water layer as a function of time. After 3 h of centrifugation, the layer appears above a critical SDS concentration of 0.06 M and above this threshold value the rate of coalescence increases with the SDS concentration. Although qualitative, this experiment confirms the fact that the presence of SDS molecules destabilizes the inverted films.

The surface/volume ratio is rather high for the small water droplets, and an important fraction of SDS molecules

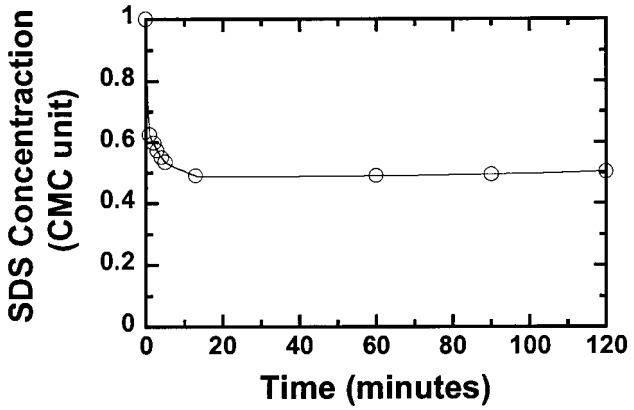

Figure 9. Evolution of the SDS concentration in the external water phase. $d_g = 2\ \mu$m, $d_i = 0.36\ \mu$m, $\phi_g = 30\%$, $\phi_i = 30\%$, $C_l = 2\%$ (w/w). Internal aqueous phase = water + glucose (11.5% (w/w)). External water phase = water + SDS + glucose (11.5% (w/w)).

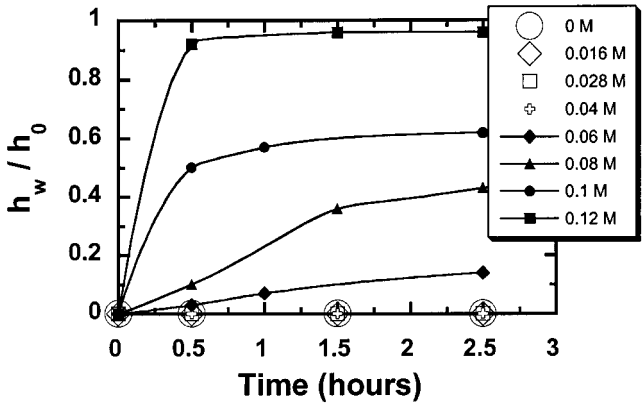

Figure 10. Evolution of the relative height h_w of coalesced water as a function of time. h_0 corresponds to the maximum height of water (if the simple emulsion is totally destroyed). $d_i = 0.36\ \mu$m, $\phi_i = 30\%$, $C_l = 2\%$ (w/w). The solid lines are guides for the eyes.

is adsorbed at the oil−water interface. We can consider that the interface is saturated in SDS when its concentration C_{hi}^{v} in the droplet volume reaches 1 cmc (=5×10^{-4} M in the presence of NaCl 0.4 M). Assuming that the surface saturation occurs at the coalescence concentration threshold ($C_{hi} = 0.06$ M), we find a SDS surface coverage of 1.7 molecules/nm^2. In other words, the inverted W/O/W films are rapidly destroyed when the SDS surface concentration is close to 1.7 molecules/nm^2. In Figure 10, the rate of coalescence increases even after the saturation value has been reached, that is, above cmc. This may appear surprising considering that the monolayer composition is not supposed to vary once the critical micellar concentration is reached. To explain this result, we suggest that the molecules dissolved in the droplet bulk play a role in the hole nucleation process. Indeed, SDS molecules can diffuse from the bulk to the positively curved part of the hole which is a preferential adsorption site. Once adsorbed, they lower the activation energy and the film lifetime decreases because of their positive spontaneous curvature (see Figure 11). Since the rate of diffusion increases with the surfactant concentration, the destruction should be accelerated as observed experimentally.

5. Kinetics of Release in Double Emulsions. The nucleation frequency ω of a hole that reaches a critical size, above which it becomes unstable and grows, determines the lifetime of the films. A mean field description[10] predicts that ω varies with temperature T as an Arrhenius law: $\omega = \omega_0 \exp(-E_a/kT)$. In this expression, kT is the thermal energy, ω_0 is the natural frequency, and E_a is the so-called activation energy, that is, the energy cost for reaching the critical hole radius. Assuming a unique rupturing frequency ω per unit film area, numerical simulations performed on a cellular material reveal that the scenario of destruction through coalescence is intrinsically catastrophic and inhomogeneous[11] with a few giant cells growing much more rapidly than the average, in agreement with the experimental observations.[12] Due to the complexity of the destruction scenario in simple emulsions, the measurements of the microscopic parameters ω_0 and E_a are scarce.[13,14]

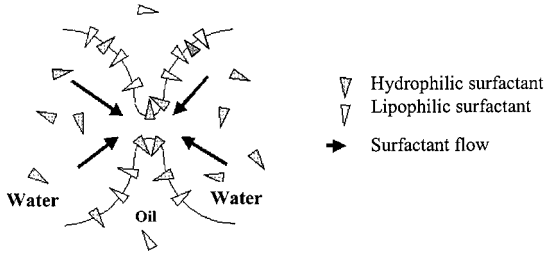

Figure 11. Scheme showing the diffusion of the high HLB surfactant toward the curved part of the hole.

In this section, by varying the hydrophilic surfactant concentration we identify and separate two release mechanisms in double emulsions. One occurs by diffusion or permeation of the salt across the oil globule. The second one involves coalescence only between the internal droplets and the globule surface. We study the kinetics of release in the regime dominated by coalescence, and we propose an unambiguous method for the measurement of the microscopic parameters ω_0 and E_a based on the use of monodisperse water-in-oil-in-water type (W/O/W) double emulsions. Our method exploits the fact that the total number of internal droplets adsorbed on the globule surface governs the rate of release. An attractive London−van der Waals interaction exists both between the small internal droplets and between the droplets and the globule surface. However, since the globules are at least 10 times larger than the entrapped droplets, the attraction between the almost flat globule surface and the small droplets is nearly twice as large as that between the inner droplets.[15] This attraction is small enough for the small droplets to behave as a gas that reversibly adsorbs onto the globule surface. At low internal droplet volume fraction, by varying the concentration of the hydrophilic surfactant we exploit the regime where the leakage is controlled only by the droplet/globule coalescence. In such conditions, measuring the rate of release allows a direct determination of the average lifetime of the thin film that forms between the small internal droplet and the globule surface. We therefore deduce the activation energy and the natural frequency of the hole nucleation process by exploring the temperature dependence of the rate of release.

a. Limit of Low SDS Concentration and Low Internal Droplet Volume Fraction. Because in the following experiments the internal water volume is about 100 times smaller than the external one, C_h sets the chemical potential of the SDS molecules. The thin liquid film that

(11) Hasmy, A.; Paredes, R.; Sonnneville-Aubrun, O.; Cabane, B.; Botet, R. *Phys. Rev. Lett.* **1999**, *82*, 3368.
(12) Bibette, J.; Morse, D. C.; Witten, T. A.; Weitz, D. A. *Phys. Rev. Lett.* **1992**, *69*, 981.
(13) Kabalnov, A.; Weers, J. *Langmuir* **1996**, *12*, 1931.
(14) de Gennes, P. G. *C. R. Acad. Sci., Ser. IIb* **1998**, *326*, 331.
(15) Israelachvili, J. N. In *Intermolecular and surface forces*; Academic Press: London, 1992.

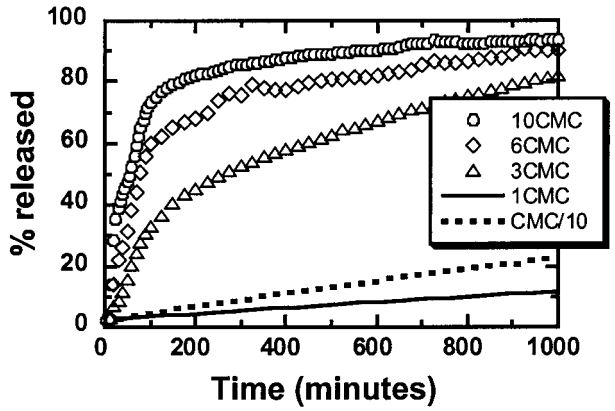

Figure 12. Influence of SDS concentration in the external water phase on the kinetics of release. $d_g = 4\ \mu m$, $d_i = 0.36\ \mu m$, $\phi_i^0 = 20\%$, $\phi_g = 10\%$.

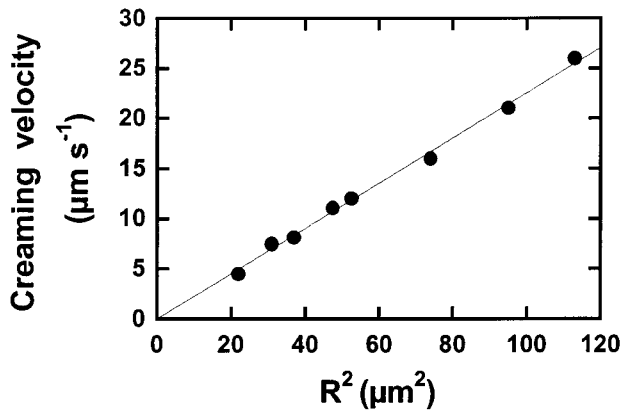

Figure 13. Creaming velocity of double globules as a function of their radius. $d_i = 0.36\ \mu m$, $\phi_i^0 = 56\%$, $C_l = 2\%$ (w/w), $C_h =$ cmc/10.

forms between the internal droplets and the globule surface is composed of two mixed monolayers covered by Span 80 and SDS molecules, separated by oil. Since SDS molecules migrate from the external to the internal water phase within a very short period of time (some minutes, see section III.3.), the film can be regarded as close to thermodynamic equilibrium with respect to surfactant adsorption a few minutes after preparation. Following the well-known Bancroft rule, such inverted films possess a long-range stability when essentially covered by hydrophobic surfactant (Span 80) but become very unstable when a strong proportion of hydrophilic surfactant is adsorbed. From the previous experiments, we learned that the transition from long-range to short-range stability may be achieved by varying the concentration of the hydrophilic surfactant in the external water phase.

Several emulsions are then prepared with 2% (w/w) of Span 80 as the emulsifier of the primary emulsion and SDS, at various concentrations C_h in the external continuous phase. Figure 12 shows the quantity of released salt (expressed in relative percentage) as a function of time. The globule diameter d_g is 4 μm, the initial droplet volume fraction ϕ_i^0 is 20%, and the globule volume ϕ_g fraction is 10%. From these curves, we can deduce that two limiting mechanisms control the salt release in double emulsions. Since they occur over time scales that are significantly different, they can be decoupled. For $C_h \leq$ cmc, the rate of release is quite slow, occurring over a characteristic time scale of several days. The rate decreases with C_h, being minimal around 1 cmc. When the process is achieved (nearly 100% released), we observe under the microscope that the water droplet concentration ϕ_i in the globules has apparently not varied. This is confirmed by the creaming technique, since we measure a constant rate of creaming of the globules after 3 days of storage. Figure 13 represents the evolution of the creaming velocity as a function of $R^2 = (d_g/2)^2$, 72 h after the sample preparation. The ϕ_i value deduced from eqs 1 and 2 corresponds to the initial one, $\phi_i^0 = 56\%$. We therefore conclude that in this regime the salt release occurs without film rupturing; instead, it is produced by an entropically driven diffusion and/or permeation of the salt across the oil globule. It is important to stress that the size invariance of the internal droplets reflects the fact that the transfer of NaCl from the internal to the external water phase occurs approximately at the same rate as the transfer of glucose from the external to the internal water phase. Indeed, the initial osmotic matching does not ensure the absence of water flow if the rates of molecular transfer are not identical.

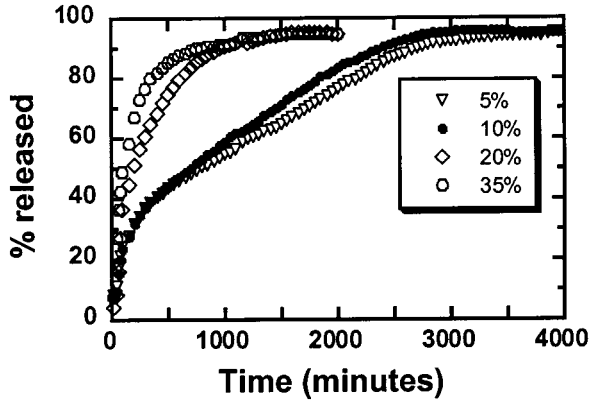

Figure 14. Influence of the initial internal droplet volume fraction on the kinetics of release. $d_g = 3.6\ \mu m$, $d_i = 0.36\ \mu m$, $\phi_g = 10\%$, $C_h = 3$ cmc.

For $C_h >$ cmc, the release is quite fast and the rate increases with the hydrophilic surfactant concentration. Repeated observations under the microscope reveal a gradual decrease of the inner droplet concentration, being almost zero when 100% of release is attained. When $C_h < 5$ cmc, we do not observe any coarsening of the water-in-oil droplets. This definitely confirms that in this SDS concentration range, the salt release is controlled by the coalescence of the internal droplets on the globule surface.

We now examine in more detail the regime governed by coalescence. In the following experiments, $C_h = 3$ cmc, $d_g = 3.6\ \mu m$, $\phi_g = 10\%$, and we vary the initial internal droplet volume fraction between 5% and 35%. In the experimental conditions and within the time scales that are explored (less than 1000 min), the contribution of diffusion/permeation across the oil globule can be neglected. The data are represented in Figure 14. A significant decay of the characteristic time of release as a function of the internal droplet volume fraction is observed. In terms of kinetics, this result rules out describing the coalescence process as a first-order reaction involving the concentration of internal droplets. At this point, we make the assumption that a fraction of the internal droplets are adsorbed on the globule surface. This is a natural consequence of the van der Waals attraction that exists between the internal droplets and the external water phase.[15] Let us define n_i as the total internal droplet concentration within the globules and n_a as the concentration of adsorbed droplets (per unit volume of the globules). We guess that the number of coalescence events per unit time is simply proportional to the concentration of adsorbed droplets:

$$dn_i/dt = -\Omega n_a \quad (3)$$

where Ω is the characteristic frequency of coalescence between an adsorbed droplet and the globule surface. At any time t, n_i is calculated from the ordinate of the curves (Figure 14) and the number of coalescence events dn_i/dt may be deduced from the derivative of the curves. All the experimental points in Figure 14 are transformed and plotted again in (n_i, dn_i/dt) coordinates in Figure 15. We observe that all the data define a single curve, which means that the rate coalescence dn_i/dt depends only on n_i. Following eq 3, this function is proportional to Ω and corresponds to the adsorption isotherm of the water droplets on the globule surface, $n_a = f(n_i)$. As n_i rises, the function should approach an asymptotic value reflecting the saturation of the globule surface by the adsorbed water droplets. On the other hand, in the low concentration limit, the rate of disappearance of droplets should become linearly proportional to droplet concentration. Between these two limits, one can expect an intermediate regime characterized by a nonlinear evolution of dn_i/dt with n_i. In Figure 14, the data for $\phi_i^0 = 5\%$ and 10% are very similar in shape. After a rapid initial rise, there is a long period of time where the release varies linearly with time until it reaches nearly 100%. The rapid rise at short times corresponds to the intermediate regime with $2\ \mu m^{-3} < n_i < 4\ \mu m^{-3}$. At longer times, the linear part of the plots (Figure 14) corresponds to the low adsorption limit ($n_i < 2\ \mu m^{-3}$). For initially concentrated globules ($\phi_i^0 = 20\%$ and 35%), a large part of the curves is dominated by the regime close to saturation or the intermediate regime ($2\ \mu m^{-3} < n_i < 10\ \mu m^{-3}$), which explains the very fast leakage observed in Figure 14. The fraction of the curve corresponding to $n_i < 2\ \mu m^{-3}$ is not distinguishable in Figure 15 due to scale of the plot. This is why we report in Figure 16 the evolution of dn_i/dt in the limit of low n_i values and for three different globule sizes, $d_g = 2$, 3.6, and 14.5 μm ($\phi_i^0 = 35\%$, $\phi_g = 10\%$, $d_i = 0.36\ \mu$m, $C_l = 2\%$, $C_h = 3$ cmc). In all cases, the evolution is linear as could be expected. For the sake of comparison, the data in the ordinate are normalized by the total number (per unit volume) of available sites for adsorption n_0, easily deduced from geometrical considerations.

We aim now to model the adsorption isotherm in order to deduce a numerical value for Ω. The presence of an inflection point on Figure 15 indicates that the curve is not "Langmuir-like" over the whole concentration range and that lateral interactions between the adsorbed droplets must be taken into account, at least for high n_i values. Following the model of Frumkin and Fowler,[16] n_a is given by the following set of equations:

$$\frac{\Theta}{1-\Theta} = K(n_i - n_a)\exp\left(-\frac{u_a + 4u_l\Theta}{kT}\right) \quad (4)$$

$$\Theta = \frac{n_a}{n_0} \quad (5)$$

where u_a is the adsorption energy, u_l is the lateral energy of interaction between the droplets, and K is a constant calculated from the model:[16]

$$K = kT\sigma\tau(2\pi mkT)^{1/2}$$

In the expression of K, σ is the area of an adsorption site (i.e., the droplet cross section), τ is the average time spent by a droplet on the globule surface during an elastic collision, and finally m is the droplet mass. τ is assumed to be the average time for an internal droplet to displace by diffusion over a characteristic distance comparable to the surfactant layer thickness. For droplets with diameter $d_i = 0.36\ \mu$m, we find $\tau = 2 \times 10^{-6}$ s.

From the average length of the surfactant tails ($l \approx 3$ nm), we get an estimation of the van der Waals interactions: $u_l \approx -Ad_i/24l = -1.75\ kT$ and $u_a \approx -Ad_i/12l = -3.5\ kT$ (for the evaluation of u_a, the globule surface is assumed to be flat, and the Hamaker constant A for the dodecane/water couple is taken to be 0.3×10^{-20} J).[15] The coalescence frequency is therefore the unique free parameter in our model and is determined from the best fit to the experimental curves. In Figure 17 is plotted the kinetic evolution of n_i at $C_h = 3$ cmc and two different globule diameters: $d_g = 3.6\ \mu$m and $d_g = 14.5\ \mu$m. Note that the release occurs faster for smaller globules: this merely reflects the fact that the accessible surface (per unit volume) for droplet adsorption varies as $1/d_g$. Using one and the same value of Ω, the theoretical points (continuous lines) correctly fit the experimental data (empty symbols): $\Omega = 6 \times 10^{-3}$ min^{-1}. From the obtained numerical value of Ω, it can be estimated that a droplet spends on average 3 h on the globule surface before a coalescence event occurs. The same type of measurement was performed in the same conditions ($C_h = 3$ cmc) but varying the oil chemical nature: we found $\Omega = 0$ min^{-1} for octane globules (no coalescence occurred) and $\Omega = 2.5 \times 10^{-2}$ min^{-1} for hexadecane. In

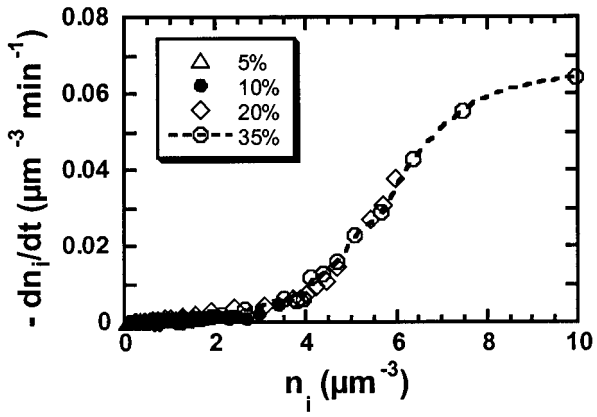

Figure 15. Rate of coalescence as a function of the number density of internal droplets in the globules. $d_g = 3.6\ \mu$m, $d_i = 0.36\ \mu$m, $\phi_g = 10\%$, $C_h = 3$ cmc, $C_l = 2\%$ (w/w). The dashed line is a guide to the eyes.

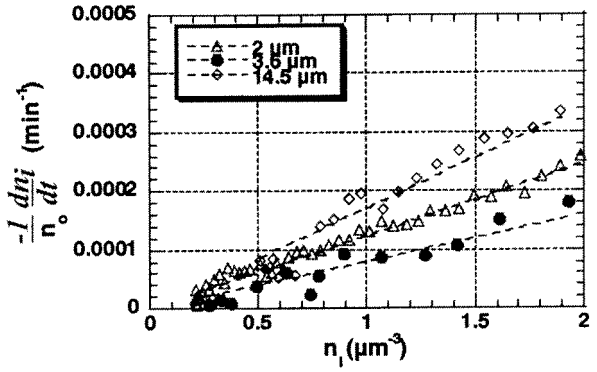

Figure 16. Rate of coalescence as a function of the number density of internal droplets in the globules. For the sake of comparison, the data in the ordinate are normalized by the total number (per unit volume) of available sites for adsorption n_0. $\phi_i^0 = 35\%$, $\phi_g = 10\%$, $d_i = 0.36\ \mu$m, $C_l = 2\%$ (w/w), $C_h = 3$ cmc. The dashed lines are guides to the eyes.

(16) Fowler, R. H.; Guggenheim, A. In *Statistical thermodynamics*; University Press: Cambridge, 1939.

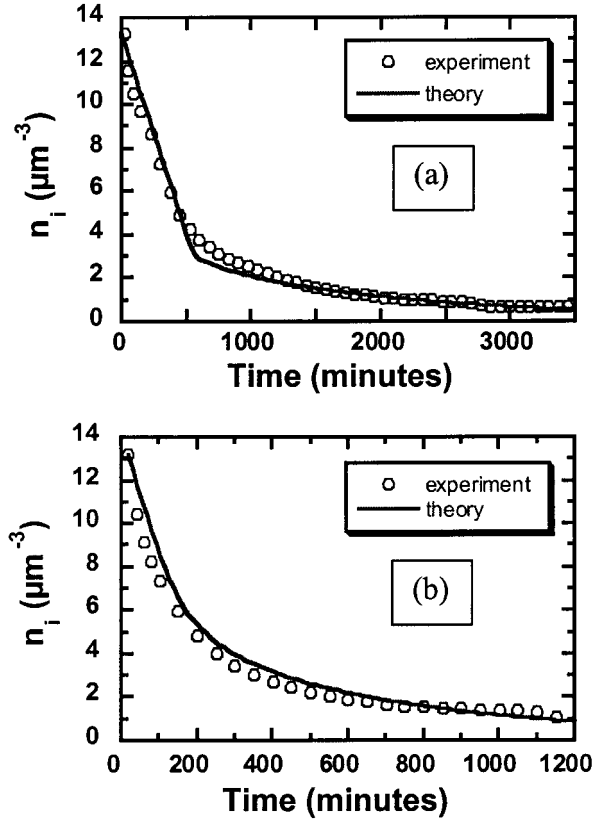

Figure 17. Number density of internal droplets in the globules as a function of time. $d_i = 0.36\ \mu$m, $\phi_i^0 = 35\%$, $\phi_g = 10\%$, $C_h =$ 3 cmc, $C_l = 2\%$ (w/w). (a) $d_g = 14.5\ \mu$m; (b) $d_g = 3.6\ \mu$m.

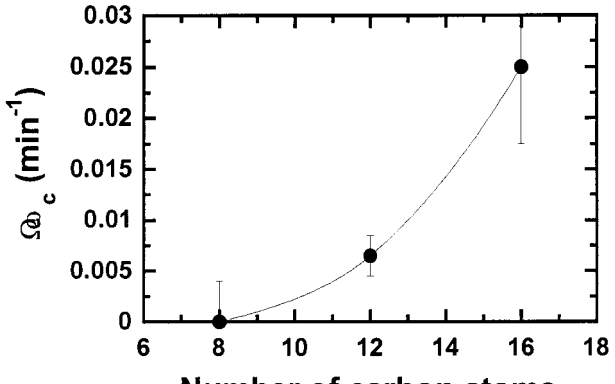

Figure 18. Evolution of the coalescence frequency Ω as a function of the oil hydrocarbon chain length. $d_g = 3.6\ \mu$m, $d_i =$ 0.36 μm, $\phi_i^0 = 20\%$, $\phi_g = 10\%$, $C_h = 3$ cmc, $C_l = 2\%$ (w/w).

Figure 18 is plotted the evolution of Ω as a function of the hydrocarbon chain length. The van der Waals energy u_a is not varying much between the three different oils[15] and does not quantitatively justify the evolution of Ω. We believe that this evolution is rather related to the spontaneous curvature of the surfactant monolayers. We suggest that the longer chain (hexadecane) can hardly penetrate the surfactant brush covering the surfaces and therefore the natural spontaneous curvature is quite elevated allowing rapid formation of holes in the W/O/W films. Instead, shorter oil chains such as octane can more easily penetrate and swell the surfactant brush providing a more negative average curvature, which stabilizes the inverted films against hole nucleation.

To confirm the validity of our procedure, the coalescence frequency was determined independently from a simple

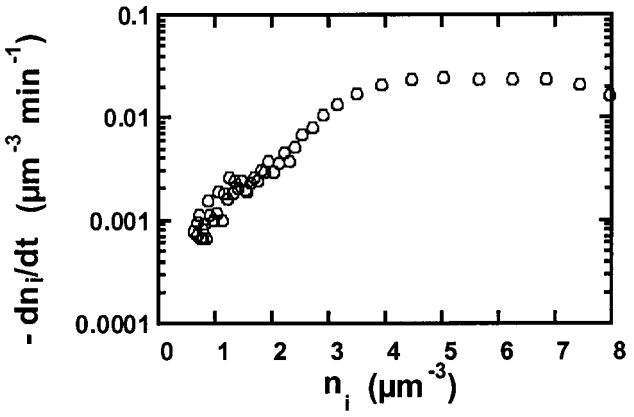

Figure 19. Rate of coalescence as a function of the number density of internal droplets in the globules. $d_g = 11.5\ \mu$m, $d_i =$ 0.36 μm, $\phi_i^0 = 25\%$, $\phi_g = 10\%$, $C_h = 3$ cmc; 0.1% of silicon oil with a gyration radius of 12 nm is added to dodecane.

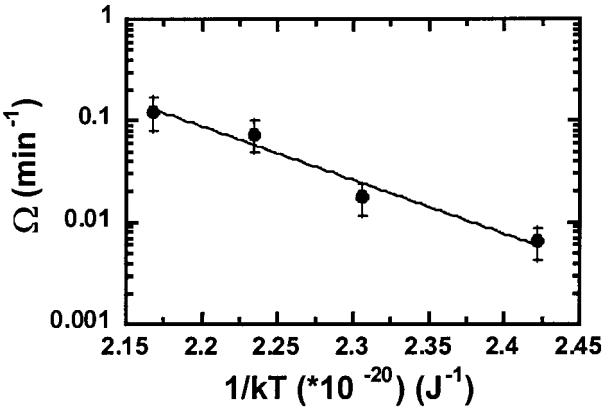

Figure 20. Frequency of coalescence as a function of $1/kT$. d_i = 0.36 μm, $\phi_i^0 = 20\%$, $\phi_g = 10\%$, $C_h = 3$ cmc, $C_l = 2\%$ (w/w).

experiment in which the globule surface was saturated by the water droplets. For that purpose, we introduce in the oil phase (dodecane) a silicon polymer that brings an additional depletion attraction to the previously mentioned van der Waals interaction.[17] We checked that this polymer does not adsorb at the water/oil interface and therefore does not perturb the film properties.[18] 0.1% of silicon oil with a gyration radius of 12 nm is sufficient to saturate the globule surface for $10\% < \phi_i < 25\%$ and $d_g = 11.5\ \mu$m. The saturation produces a spherical shell observable under the microscope. The rate of coalescence dn_i/dt remains constant as long as the globule surface is saturated, and this is confirmed by the appearance of a plateau in Figure 19. Dividing the plateau value by the total concentration of available sites for adsorption (calculated from simple geometrical considerations), we obtain $\Omega = 5 \times 10^{-3}$ min^{-1}, in very good agreement with the value deduced from Frumkin−Fowler's model.

To determine the activation energy E_a and the hole natural frequency, we vary the temperature between 15 and 60 °C, all other parameters being constant. In Figure 20, we show the evolution of ln(Ω) as a function of $1/kT$ for the system SDS/Span 80/dodecane with $d_i = 0.36\ \mu$m. From the best fit to our data (solid line), we get $E_a = 30$ kT_r, T_r being the room temperature (25 °C). From the intercept, we obtain $\Omega_0 = 4 \times 10^{10}$ min^{-1}. The ratio Ω(25 °C)/Ω_0 is roughly equal to 10^{13} meaning that only one hole

(17) Pays, K.; Leal-Calderon, F.; Mondain Monval, O.; Bibette, J. *Langmuir* **1997**, *13*, 7008.

(18) Pays, K. Double emulsions: coalescence and compositional ripening. Ph.D. Thesis, University Bordeaux 1, 2000.

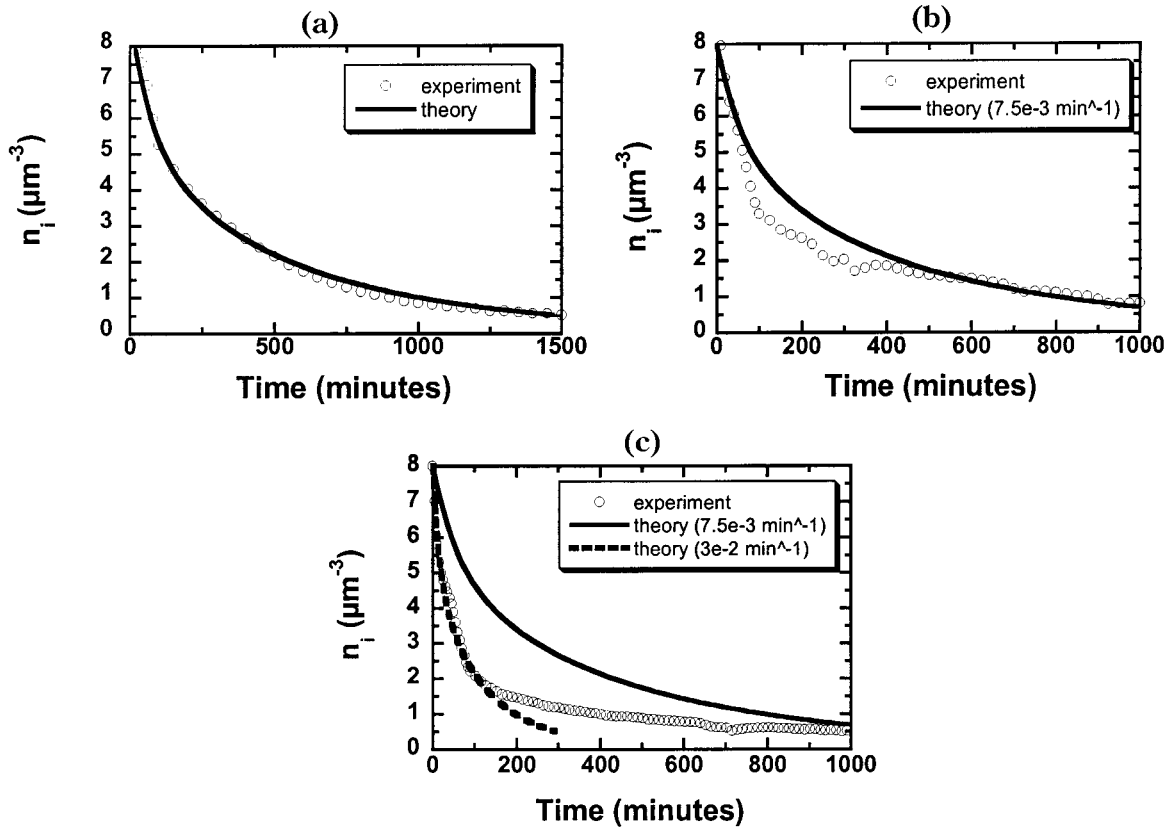

Figure 21. Number density of internal droplets in the globules as a function of time. $d_g = 3.6\ \mu$m, $d_i = 0.36\ \mu$m, $\phi_i^0 = 20\%$, $\phi_g = 12\%$, $C_l = 2\%$ (w/w). (a) $C_h = 3$ cmc; (b) $C_h = 6$ cmc; (c) $C_h = 10$ cmc. In the insets, the numbers correspond to the Ω values tested to fit the experimental data.

over 10^{13} grows and ultimately produces a coalescence event. Since the contact area a_0 between the droplets and the globule surface lies between 10 and 100 nm^2, we deduce a frequency ω_0 per unit film area of the order of $10^{25}-10^{26}$ m^2 s^{-1}. The same order of magnitude is obtained from dimensionality arguments, assuming that the natural frequency is controlled by the viscous flow at the neck of the growing hole:[19] $\omega_0 \propto \gamma/(\eta a_0^{3/2})$, where γ ($\sim 10^{-4}$ N/m) is the measured surface tension and η (10^{-3} Pa s) is the viscosity of the continuous phase (in the previous equation, the critical hole radius is assumed to be equal to the radius of the contact area).

b. Limit of High SDS Concentration or High Internal Droplet Volume Fraction. In Figure 21, we illustrate the effect of varying the hydrophilic surfactant concentration from 3 cmc to 10 cmc. Here also, cmc refers to the critical micellar concentration of SDS in pure water. It is clear from the graph that increasing the hydrophilic surfactant concentration has the effect of accelerating the salt release.

To explain this result, one may invoke the possible solubilization of Span 80 by SDS micelles: due to the transfer of Span 80 to the external water phase, the inverted films should become unstable and the release should result from droplet−globule coalescence. This hypothesis does not seem very realistic regarding the very low solubility of Span 80 in a water phase even in the presence of SDS micelles.[9] To definitely rule out this hypothesis, we performed experiments in which the external water phase was saturated by Span 80. The obtained results were absolutely identical to the ones obtained in Figure 21.

We can also argue that the microscopic parameters Ω_0 and E_a are sensitive to the SDS surfactant concentration. Indeed, as previously described (section III.5.), the stability of simple W/O emulsions is clearly affected by SDS concentration even above its cmc value. We then try to fit the experimental curves with our adsorption−coalescence model, using Ω as unique free parameter. As can be observed in Figure 21, the agreement between theory and experiment is fairly good at 3 cmc but large deviations appear at higher SDS concentrations. In Figure 21c, two different Ω values are probed to fit the experimental data but neither of them is satisfactory. From this, we conclude that the model valid at low SDS concentrations is not correctly describing the experimental results at high SDS concentrations. In other words, the rate of release can no longer be described in terms of a unique coalescence frequency when SDS concentration is higher than about 5 cmc. We guess that at such high concentrations, droplet−droplet coalescence accelerates the rate of release. Indeed, internal droplet coalescence produces large nuclei which are preferentially adsorbed on the globule surface due to their larger van der Waals attraction. Moreover, when a nucleus coalesces at the globule surface, a larger amount of matter is released at a time. The inherent polydispersity resulting from droplet−droplet coalescence can therefore explain the complex behavior of highly concentrated SDS double emulsions and the fact that the process cannot be described using a single coalescence frequency. The same type of conclusion can be established when the initial internal droplet concentration is large, even at low surfactant concentration. As is evident in Figures 6 and 7, droplet−droplet coalescence is taking place and accelerates the rate of destruction.

(19) Deminière, B.; Colin, A.; Leal-Calderon, F.; Bibette, J. *Phys. Rev. Lett.* **1999**, *82*, 229.

IV. Conclusion

In this paper, the general phenomenology for the release of a double emulsion stabilized by short surfactants has been described. By appropriately choosing the surfactant concentrations as well as their chemical nature, we were able to dissociate the two mechanisms that are responsible for the release of chemical substances. This allowed us to study the stability toward coalescence of mixed surfactant films, that is, films stabilized by both water and oil-soluble surfactants. From a practical point of view, we can conclude that long-term encapsulation of small neutral or charged molecules is not really possible using short surfactants as stabilizing agents. Indeed, when the hydrophilic surfactant concentration is lower than a critical value C_h*, the release occurs preferentially by diffusion and/or permeation across the oil phase, while above C_h* it occurs preferentially by coalescence. In both cases, the characteristic period of release does not exceed several days, which is not sufficient for most of the practical applications. C_h* is of the order of 1 cmc for highly hydrophilic surfactants (HLB > 30) and 100 cmc for lower HLB surfactants (10 < HLB < 30).[9] Because of the inefficiency of short surfactants, much effort is being spent in finding formulations incorporating polymeric stabilizers[20] or associating short surfactants and polymers or proteins.[21] It is indeed expected that the presence of large molecules at the interfaces will reduce the inner droplet adsorption on the globule surface and increase the activation energy for the hole nucleation process. Promising results have already been empirically obtained,[21] but there is still work to be done to perfectly control and understand the release properties of these new materials as well as to ensure their reliability as commercial products.

Acknowledgment. The authors gratefully acknowledge the FOURNIER Company for financial support.

LA010735X

(20) Sela, Y.; Magdassi, S.; Garti, N. *Colloids Surf.* **1993**, *83*, 143.
(21) Garti, N.; Aserin, A.; Cohen, Y. *J. Controlled Release* **1994**, *29*, 41.